DSS1 Restrains dsDNA Engagement of BRCA2 to Promote Homologous Recombination and Impact Replication Fork Stability and R-loop Homeostasis

Yuxin Huang[1,9], Wenjing Li[1,9], Tzeh Foo[2], Jae-Hoon Ji[1,3], Bo Wu[1], Nozomi Tomimatsu[4], Qingming Fang[1,3], Boya Gao[5], Melissa Long[5], Jingfei Xu[6], Rouf Maqbool[1], Bipasha Mukherjee[2], Tengyang Ni[1], Salvador Alejo[7], Yuan He[6], Sandeep Burma[1,4], Li Lan[5,8], Bing Xia[2], and Weixing Zhao[1,3]*

[1]Department of Biochemistry and Structural Biology, University of Texas Health and Science Center, San Antonio, Texas, 78229, USA

[2]Department of Radiation Oncology, Rutgers Cancer Institute of New Jersey and Robert Wood Johnson Medical School, New Brunswick, NJ 08903, USA

[3]Greehey Children's Cancer Research Institute, University of Texas Health Science Center at San Antonio, San Antonio, TX 78229, USA.

[4]Department of Neurosurgery, University of Texas Health Science Center at San Antonio, San Antonio, TX 78229, USA.

[5]Department of Radiation Oncology, Massachusetts General Hospital, Harvard Medical School, Boston, MA 02129

[6]Department of Molecular Biosciences, Northwestern University, Evanston, IL, USA.

[7]Department of Obstetrics & Gynecology, University of Texas Health Science Center, San Antonio, TX 78229, USA

[8]Department of Molecular Genetics and Microbiology, School of Medicine, Duke University, Durham, NC 27710, USA

[9]These authors contributed equally to this work

* Corresponding author. Email: zhaow2@uthscsa.edu

Includes:
Supplementary Figures 1 through 12

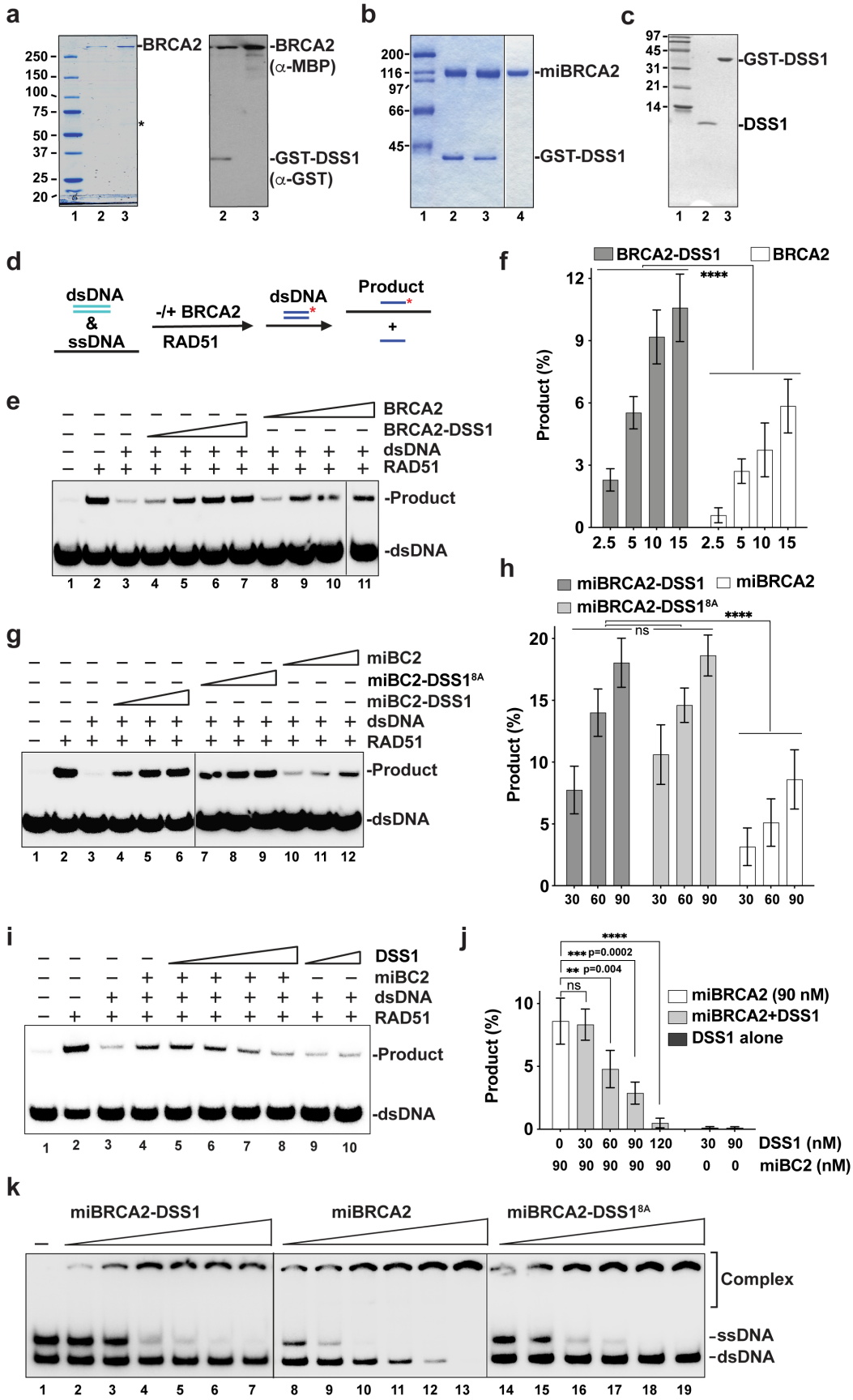
a
BRCA2
BRCA2 (α-MBP)
GST-DSS1 (α-GST)
b
miBRCA2
GST-DSS1
c
GST-DSS1
DSS1
d
dsDNA & ssDNA
-/+ BRCA2 RAD51
dsDNA
Product
e
BRCA2
BRCA2-DSS1
dsDNA
RAD51
-Product
-dsDNA
f
BRCA2-DSS1
BRCA2
Product (%)
****
g
miBC2
miBC2-DSS1^8A
miBC2-DSS1
dsDNA
RAD51
-Product
-dsDNA
h
miBRCA2-DSS1
miBRCA2
miBRCA2-DSS1^8A
ns
****
Product (%)
i
DSS1
miBC2
dsDNA
RAD51
-Product
-dsDNA
j
****
*** p=0.0002
** p=0.004
ns
miBRCA2 (90 nM)
miBRCA2+DSS1
DSS1 alone
Product (%)
DSS1 (nM)
miBC2 (nM)
k
miBRCA2-DSS1
miBRCA2
miBRCA2-DSS1^8A
Complex
-ssDNA
-dsDNA

Supplementary Fig. 1. DSS1 facilitates BRCA2 in targeting RAD51 onto ssDNA over dsDNA. (See also Fig. 1)

a. SDS-Page of purified full length MBP-BRCA2-GST-DSS1 (lane 2) and MBP-BRCA2 (lane 3) (left), and western blot detection of MBP-BRCA2 and GST-DSS1 by antibodies against MBP and GST respectively (right). Lane 1 shows MW markers. Source data are provided as a Source Data file.

b. SDS-Page of purified miBRCA2-DSS1^{8A} (lane 2), miBRCA2-DSS1^{WT} (lane 3) and miBRCA2 (lane 4; from another gel). Lane 1 shows MW markers. Source data are provided as a Source Data file.

c. SDS-Page of purified DSS1 (lane 2) and GST-DSS1 (lane 3). Lane 1 shows MW markers. Source data are provided as a Source Data file.

d. Schematic of homologous paring assay in the presence of non-homologous dsDNA in the mixture of ssDNA to check RAD51 loading on ssDNA over dsDNA.

e. Purified BRCA2-DSS1 (2.5nM, 5nM, 10nM and 15nM, lanes 4-7), and BRCA2 (2.5nM, 5nM, 10nM and 15nM, lanes 8-11) were tested in homologous paring reactions in the presence of non-homologous dsDNA in the mixture of ssDNA at 65 mM KCl condition. Source data are provided as a Source Data file.

f. Quantification (mean ± SD) of the homologous pairing product from three independent experiments shown in Supplementary Fig. 1e. P values were calculated using two-way ANOVA for group comparison. **** P≤0.0001. p-value between BRCA2-DSS1 group and BRCA2 group is <0.0001. Source data are provided as a Source Data file.

g. Purified miBRCA2-DSS1 (30nM, 60nM and 90nM, lanes 4-6), miBRCA2-DSS1^{8A} (30nM, 60nM and 90nM, lanes 7-9), and miBRCA2 (30nM, 60nM and 90nM, lanes 10-12) were tested in homologous paring reactions in the presence of non-homologous dsDNA in the mixture of ssDNA at 65 mM KCl condition. Source data are provided as a Source Data file.

h. Quantification (mean±SD) of the homologous pairing product from three independent experiments shown in Supplementary Fig. 1g. P values were calculated using two-way ANOVA for group comparison. ns, not significant and **** P≤0.0001. p-value between miBRCA2-DSS1 group and miBRCA2 group is <0.0001, p-value between miBRCA2-DSS1 group and miBRCA2-DSS18A group is 0.89. Source data are provided as a Source Data file.

i. Purified miBRCA2-DSS1 (90nM, lanes 4), miBRCA2 (90nM) with increased amount of DSS1 (30nM, 60nM, 90nM and 120nM; lanes 5-8) or DSS1 alone (30nM and 90nM, lanes 9-10) were tested in homologous paring reactions in the presence of non-homologous dsDNA in the mixture of ssDNA at 45 mM KCl condition. Source data are provided as a Source Data file.

j. Quantification (mean ± SD) of the homologous pairing product from three independent experiments shown in Supplementary Fig. 1i. Ordinary one-way ANOVA with Dunnett's post hoc test. ns, not significant, ** P ≤ 0.01 and **** P≤0.0001. p-value between miBRCA2 (90nM) and miniBRCA2+DSS1 (30nM) is 0.79, p-value between miBRCA2 (90nM) and miniBRCA2+DSS1 (60nM) is 0.0042, p-value between miBRCA2 (90nM) and miniBRCA2+DSS1 (90nM) is 0.0002, p-value between miBRCA2 (90nM) and miniBRCA2+DSS1 (120nM) is <0.0001. Source data are provided as a Source Data file.

k. Representative gel of dsDNA and ssDNA binding by miBRCA2-DSS1 (lanes 2-7), miBRCA2 (lanes 8-13) and miBRCA2-SS1^{8A} (lanes 14-19) at 90 mM KCl condition from three independent experiments. Source data are provided as a Source Data file.

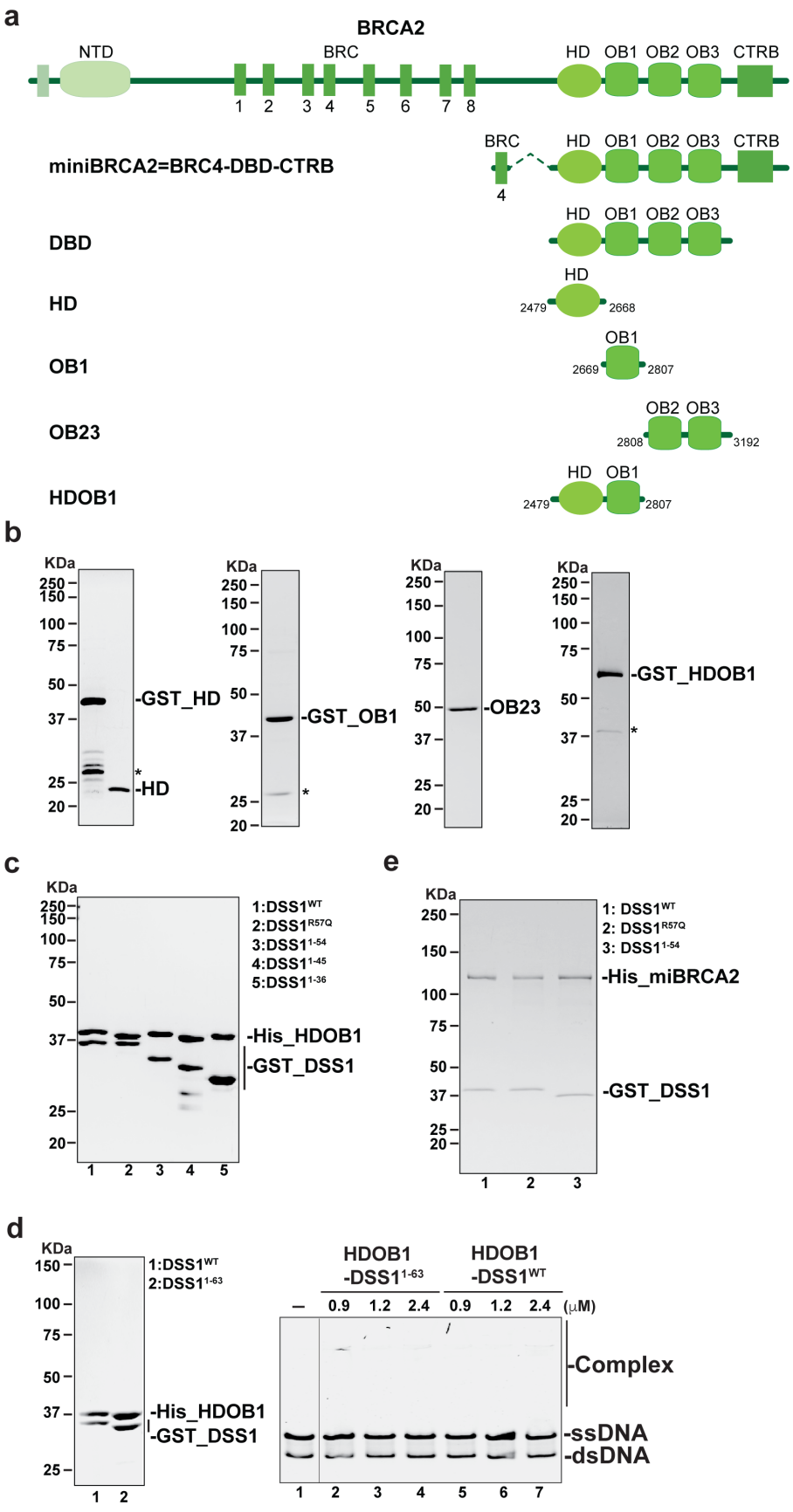
a
BRCA2
NTD
BRC
HD OB1 OB2 OB3 CTRB
1 2 3 4 5 6 7 8
miniBRCA2=BRC4-DBD-CTRB
DBD
HD
OB1
OB23
HDOB1
2479 2668
2669 2807
2808 3192
b
KDa
-GST_HD
-HD
-GST_OB1
-OB23
-GST_HDOB1
c
1:DSS1WT
2:DSS1R57Q
3:DSS1 1-54
4:DSS1 1-45
5:DSS1 1-36
-His_HDOB1
-GST_DSS1
e
1: DSS1WT
2: DSS1R57Q
3: DSS1 1-54
-His_miBRCA2
-GST_DSS1
d
1:DSS1WT
2:DSS1 1-63
HDOB1 -DSS1 1-63
HDOB1 -DSS1WT
– 0.9 1.2 2.4 0.9 1.2 2.4 (μM)
-Complex
-ssDNA
-dsDNA

Supplementary Fig. 2. Protein Purified and Used in the Study. (See also Fig. 2)
a. Schematic of BRCA2, miBRCA2 (i.e., BRC4-DBD-CTRB), DBD, HD, OB1, OB23, and HDOB1.
b. SDS-Page of purified GST-HD, HD, GST-OB1, OB23 and GST-HDOB1. Source data are provided as a Source Data file.
c. SDS-Page of purified His-HDOB1 in complex with DSS1 variants ($DSS1^{WT}$, $DSS1^{R57Q}$, $DSS1^{1-54}$, $DSS1^{1-45}$ and $DSS1^{1-36}$). Source data are provided as a Source Data file.
d. SDS-Page of purified His-HDOB1 in complex with DSS1 variants ($DSS1^{WT}$ and $DSS1^{1-63}$) and both the ds/ssDNA binding of HDOB1-$DSS1^{1-63}$ (lanes 2-4), HDOB1-$DSS1^{WT}$ (lanes 5-7). Source data are provided as a Source Data file.
e. SDS-Page of purified miBRCA2 in complex with DSS1 variants ($DSS1^{WT}$, $DSS1^{R57Q}$ and $DSS1^{1-54}$). Source data are provided as a Source Data file.

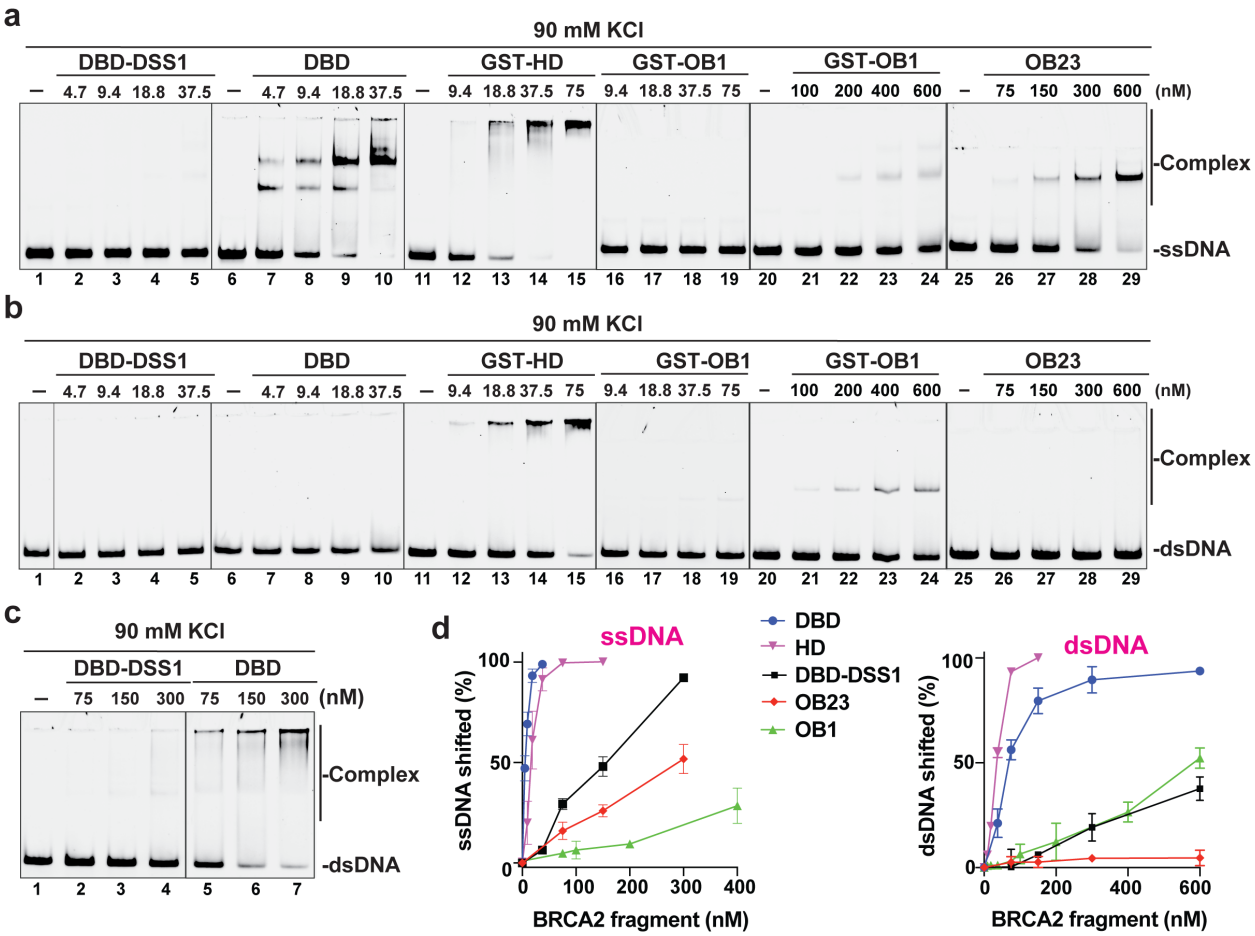

e

The apparent dissociation constant (Kd) for DNA binding of DBD fragments and DBD-DSS1 complexes

Substrate	Protein	Kd (nM)	
		90mM KCl	360mM KCl
ssDNA (80nt)	DBD	6 ± 1	
	HD (GST-tag)	15 ± 4	
	OB1 (GST-tag)	586 ± 24	
	OB23	270 ± 38	
	HDOB1 (GST-tag)	8 ± 2	
	HDOB1-DSS1$^{1\text{-}36}$ (GST-tag)	10 ± 3	
	DBD-DSS1$^{1\text{-}36}$	5 ± 1	
	DBD-DSS1^{WT}	155 ± 15	184 ± 21
	DBD-DSS1$^{1\text{-}54}$	155 ± 22	55 ± 9
	DBD-DSS1^{R57Q}	110 ± 16	61 ± 13
dsDNA (80bp)	DBD	65 ± 6	
	HD (GST-tag)	34 ± 7	
	OB1 (GST-tag)	500 ± 29	
	OB23	n.q.	
	HDOB1 (GST-tag)	18 ± 2	
	HDOB1-DSS1$^{1\text{-}36}$ (GST-tag)	32 ± 8	
	DBD-DSS1$^{1\text{-}36}$	15 ± 3	
	DBD-DSS1^{WT}	780 ± 61	n.q.
	DBD-DSS1$^{1\text{-}54}$	812 ± 32	830 ± 64
	DBD-DSS1^{R57Q}	640 ± 50	860 ± 42

Supplementary Fig. 3. DNA Binding Abilities of DBD and Its Various Domains, and Regulation of HDOB1's DNA Interaction by DSS1. (See also Fig. 2)

a. Representative gel of ssDNA (5 nM) binding by DBD-DSS1 (lanes 2-5), DBD (lanes 7-10), HD (lanes 12-15), OB1 (lanes 16-19 and 21-24) and OB23 (lanes 26-29) at 90 mM KCl condition from three independent experiments. Source data are provided as a Source Data file.

b. Representative gel of dsDNA (5 nM) binding by DBD-DSS1 (lanes 2-5), DBD (lanes 7-10), HD (lanes 12-15), OB1 (lanes 16-19 and 21-24) and OB23 (lanes 26-29) at 90 mM KCl condition from three independent experiments. Source data are provided as a Source Data file.

c. Representative gel of dsDNA (5 nM) binding by DBD-DSS1 (lanes 2-4) and DBD (lanes 5-7) with higher protein concentration (75 nM, 150 nM and 300 nM) in the assays at 90 mM KCl condition from three independent experiments. Source data are provided as a Source Data file.

d. Quantification (mean ± SD) of ssDNA binding shown in Supplementary Fig. 3a (left) and of dsDNA binding shown in Supplementary Fig. 3b and c (right). Source data are provided as a Source Data file.

e. Summary of the apparent dissociation constant (Kd) for ssDNA and dsDNA binding by various DBD fragments and DBD-DSS1 complexes tested at 90 or 360mM KCl condition.

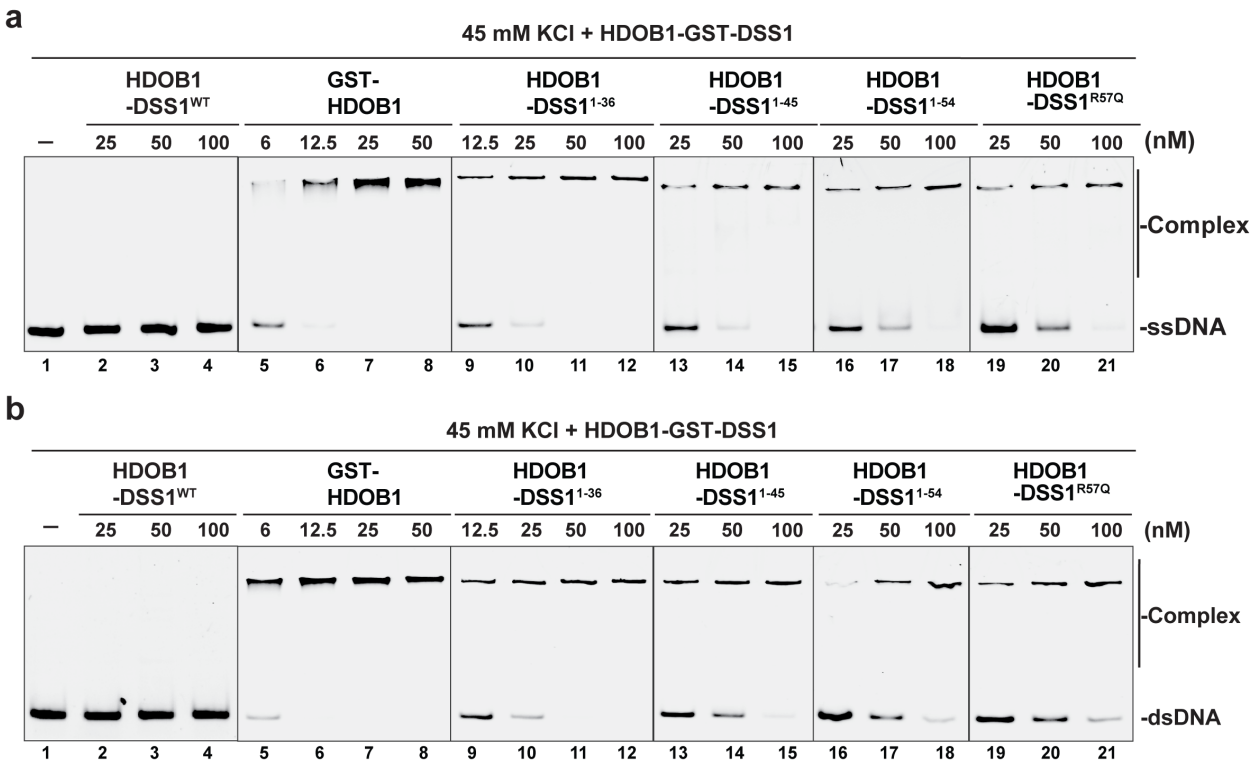

c

The apparent dissociation constant (Kd) for DNA binding of HDOB1-DSS1 complexes

Substrate	Protein	Kd (nM)
		45mM KCl
ssDNA (80nt)	HDOB1 (GST-tag)	6 ± 1
	HDOB1-DSS1$^{1-36}$ (GST-tag)	9 ± 2
	HDOB1-DSS1$^{1-45}$ (GST-tag)	24 ± 3
	HDOB1-DSS1$^{1-54}$ (GST-tag)	31 ± 4
	HDOB1-DSS1^{R57Q} (GST-tag)	40 ± 6
	HDOB1-DSS1^{WT} (GST-tag)	n.q.
dsDNA (80bp)	HDOB1 (GST-tag)	6 ± 2
	HDOB1-DSS1$^{1-36}$ (GST-tag)	17 ± 3
	HDOB1-DSS1$^{1-45}$ (GST-tag)	41 ± 2
	HDOB1-DSS1$^{1-54}$ (GST-tag)	51 ± 8
	HDOB1-DSS1^{R57Q} (GST-tag)	52 ± 9
	HDOB1-DSS1^{WT} (GST-tag)	n.q.

Supplementary Fig. 4. DNA Binding of HDOB1 and HDOB1/DSS1 complex (See also Fig. 2)
a. Representative gel of ssDNA (5nM) binding by HDOB1-DSS1^{WT} (lanes 2-4), HDOB1 (lanes 5-8), HDOB1-DSS1$^{1-36}$ (lanes 9-12), HDOB1-DSS1$^{1-45}$ (lanes 13-15), HDOB1-DSS1$^{1-54}$ (lanes 16-18) and HDOB1-DSS1^{R57Q} (lanes 19-21) at 45 mM KCl condition from three independent experiments. Source data are provided as a Source Data file.
b. Representative gel of dsDNA (5nM) binding by HDOB1-DSS1^{WT} (lanes 2-4), HDOB1 (lanes 5-8), HDOB1-DSS1$^{1-36}$ (lanes 9-12), HDOB1-DSS1$^{1-45}$ (lanes 13-15), HDOB1-DSS1$^{1-54}$ (lanes

16-18) and HDOB1-DSS1^{R57Q} (lanes 19-21) at 45 mM KCl condition from three independent experiments. Source data are provided as a Source Data file.
c. Summary of the apparent dissociation constant (Kd) for ssDNA and dsDNA binding by HDOB1 and HDOB1-DSS1 complexes tested at 45 mM KCl condition (Supplementary Fig.4a, b).

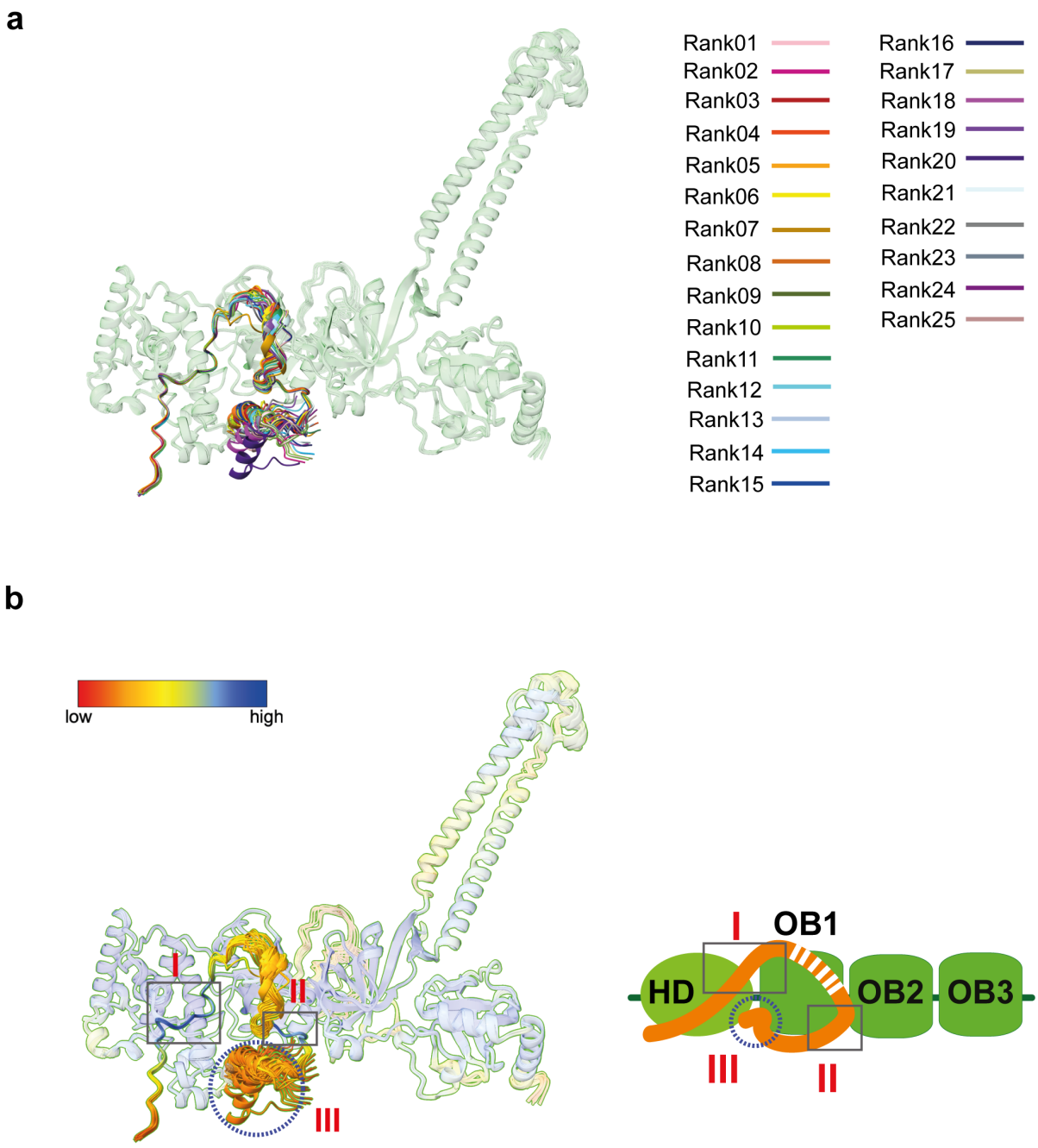

Supplementary Fig. 5. Alphafold2 multimer prediction of DBD-DSS1^{WT} (See also Fig. 1-2)
a. The top 25 ranked predictions of DBD-DSS1^{WT} are superimposed by aligning the DBD. The DBDs are shown in transparent green and the DSS1s are indicated by different colors.

b. The same superimposition above is colored by the per-residue confidence score (pLDDT; predicted Local Distance Difference Test). The three potential interfaces (I, II and II) are highlighted (left). Schematic representation of DBD- DSS1^{WT} with three interfaces and various functional domains (right) is used in the study.

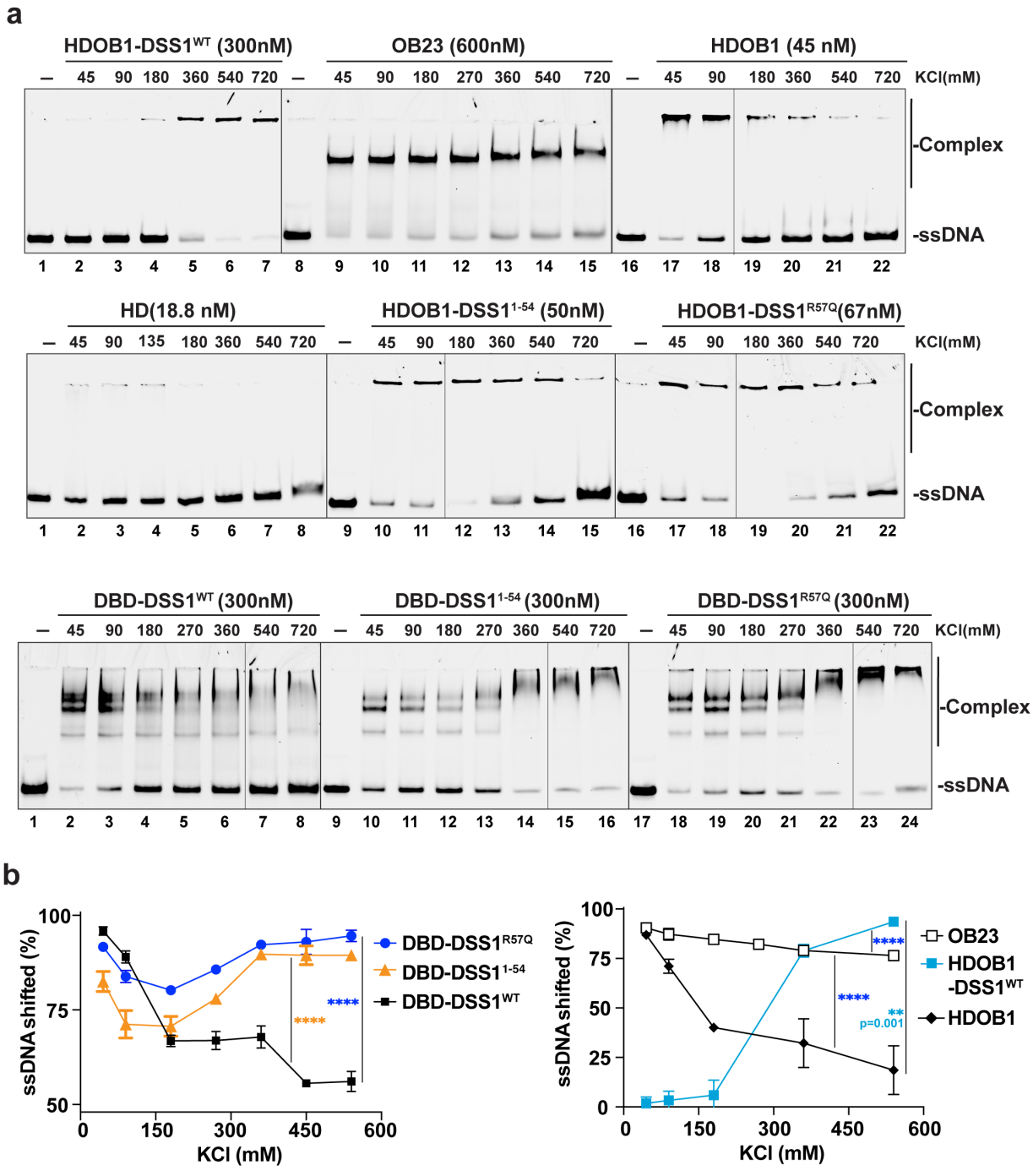

Supplementary Fig. 6. Characterization of ssDNA Binding under Increased KCl Concentration (See also Fig. 2-3)

a. Representative gel of ssDNA (5 nM) binding by HDOB1-DSS1^{WT} (lanes 2-7), OB23 (lanes 9-15), and HDOB1 (lanes 17-22) under increasing salt condition (top panel, from 45 mM to 720 mM KCl). Binding of ssDNA by HD (lanes 2-8), HDOB1-DSS1$^{1-54}$ (lanes 10-15) and HDOB1-DSS1^{R57Q} (lanes 17-22) under increasing salt condition (middle panel, from 45 mM to 720 mM KCl). Binding of ssDNA by DBD-DSS1^{WT} (lanes 2-8), DBD-DSS1$^{1-54}$ (lanes 10-16) and DBD-DSS1^{R57Q} (lanes 18-24) under increasing salt condition (bottom panel, from 45 mM to 720 mM KCl). Source data are provided as a Source Data file.
b. The corresponding quantification data (mean ± SD) were plotted to show the binding tendency in a salt-dependent manner from at least two independent experiments shown in Supplementary Fig. 6a. P values were calculated using two-way ANOVA for group comparison and Dunnett's multiple comparisons test. ** $P \leq 0.01$ and **** $P \leq 0.0001$. p-value between DBD-DSS1^{WT} and DBD-DSS1$^{1-54}$ is < 0.0001, p-value between DBD-DSS1^{WT} and DBD-DSS1^{R57Q} is < 0.0001. p-value between HDOB1 and HDOB1-DSS1^{WT} is 0.001, p-value between HDOB1 and OB23 is <0.0001, p-value between HDOB1-DSS1^{WT} and OB23 is <0.0001. Source data are provided as a Source Data file.

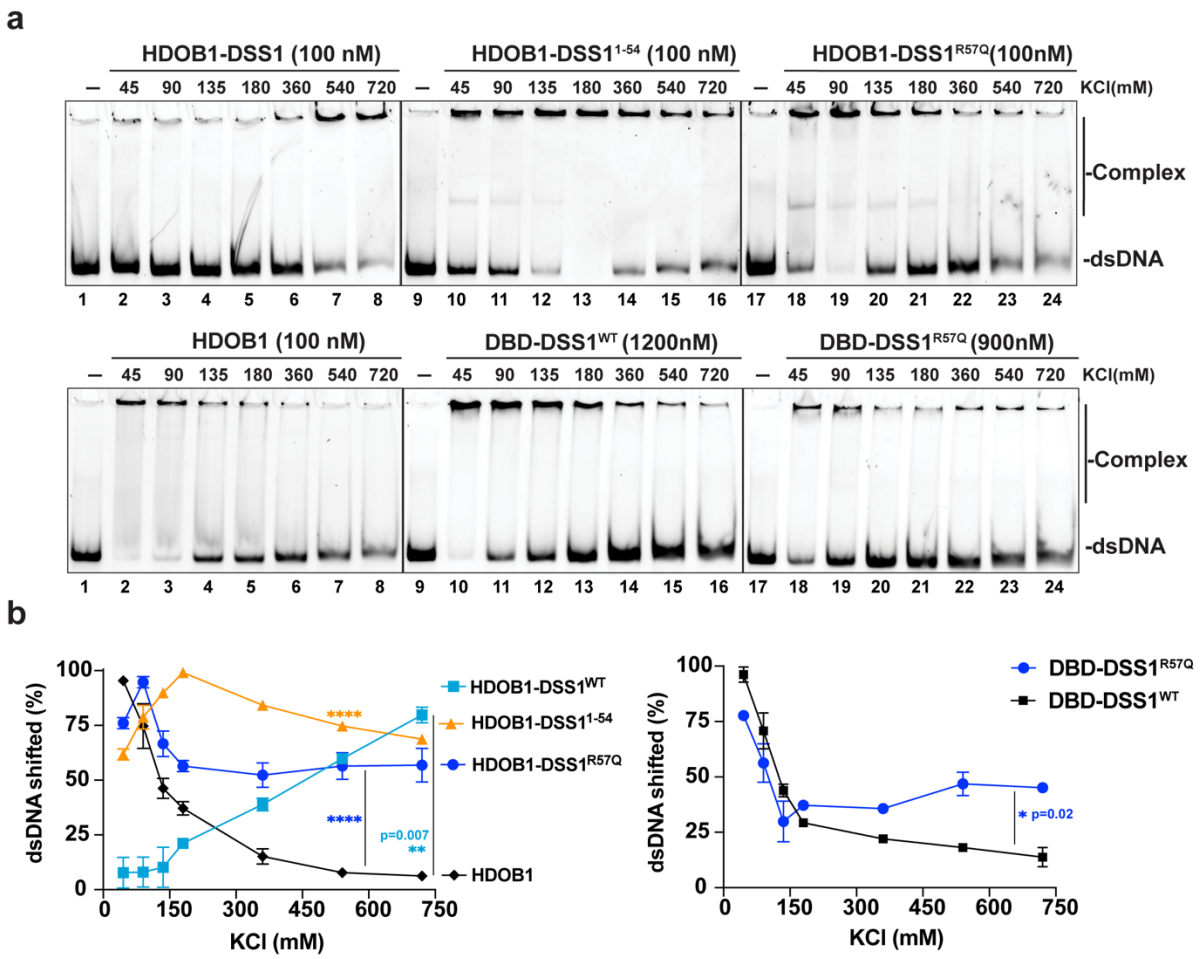

Supplementary Fig. 7. Characterization of dsDNA Binding under Increased KCl Concentration (See also Fig. 2-3)

a. Representative gel of dsDNA (5 nM) binding by HDOB1-DSS1^{WT} (lanes 2-8), HDOB1-DSS1$^{1-54}$ (lanes 10-16) and HDOB1-DSS1^{R57Q} (lanes 18-24) under increasing salt condition (top panel, from 45 mM to 720 mM KCl). Binding of dsDNA by HDOB1 (lanes 2-8), DBD-DSS1^{WT} (lanes 10-16) and DBD-DSS1^{R57Q} (lanes 18-24) under increasing salt condition (middle panel, from 45 mM to 720 mM KCl). Binding of ssDNA by DBD-DSS1^{WT} (lanes 2-8), DBD-DSS1$^{1-54}$ (lanes 10-16) and DBD-DSS1^{R57Q} (lanes 18-24) under increasing salt condition (bottom panel, from 45 mM to 720 mM KCl). Source data are provided as a Source Data file.

b. The corresponding quantification data (mean ± SD) were plotted to show the binding tendency in a salt-dependent manner from at least two independent experiments shown in Supplementary Fig. 7a. P values were calculated using two-way ANOVA for group comparison. * $P \leq 0.05$, ** $P \leq 0.01$ and **** $P \leq 0.0001$. p-value between HDOB1 and HDOB1-DSS1^{WT} is 0.0068, p-value between HDOB1 and HDOB1-DSS1$^{1-54}$ is <0.0001, p-value between HDOB1 and HDOB1-DSS1^{R57Q} is <0.0001. p-value between DBD-DSS1^{WT} and DBD-DSS1^{R57Q} is 0.015. Source data are provided as a Source Data file.

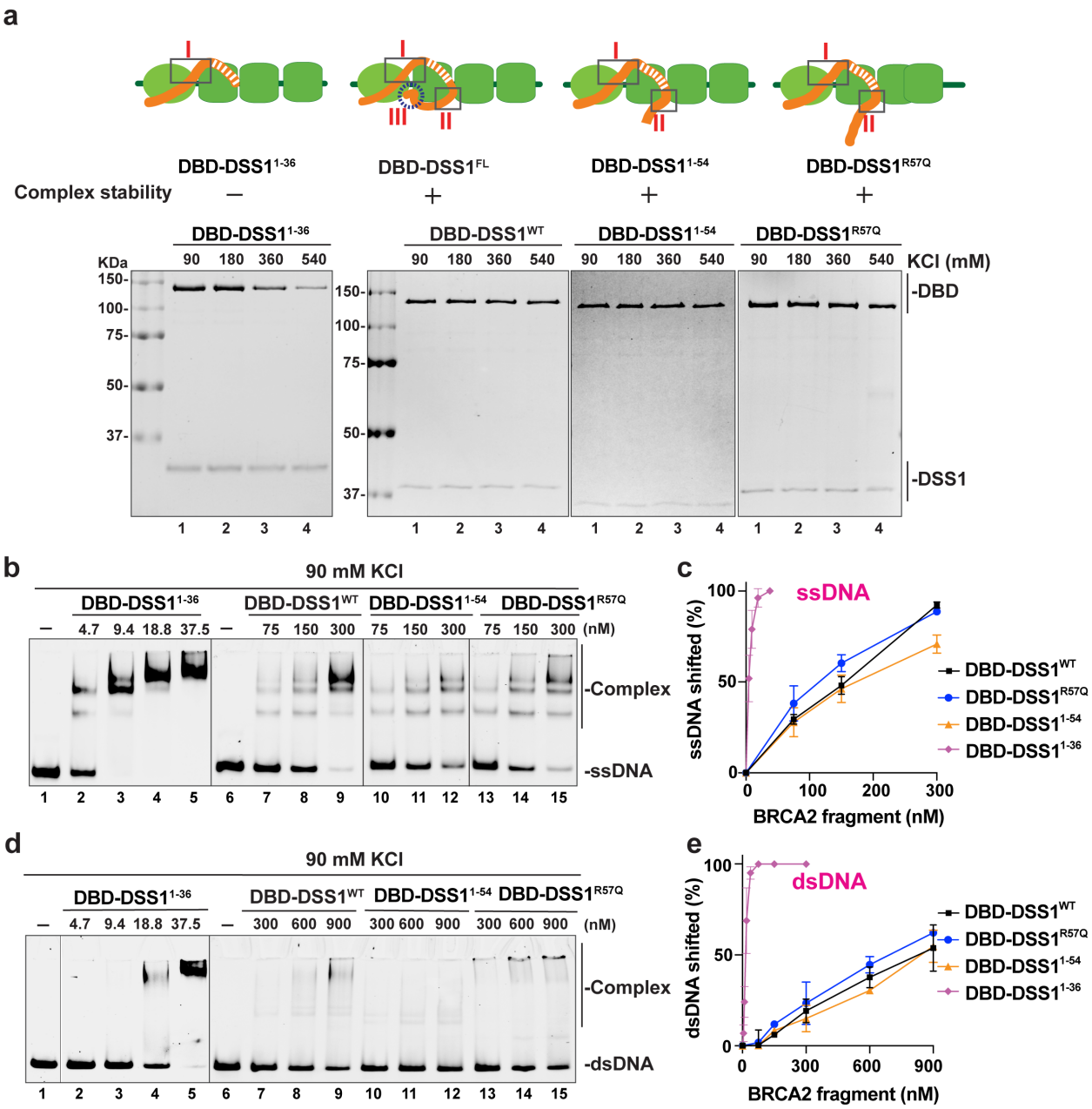

Supplementary Fig. 8. DNA Binding and Complex Formation of DBD with DSS1 or Mutants. (See also Fig. 3)

a. Schematic of the interfaces between DBD and DSS1 along with the configuration states of various DBD-DSS1 complexes hypothesized in this study (top). The complex stability is summarized (middle). The Representative SDS-Page reflecting various DBD-DSS1 complexes' stability subjected to increasing salt concentrations are shown via GST pull-down assay (bottom). Source data are provided as a Source Data file.

b. Representative gel of ssDNA (5 nM) binding by purified DBD-DSS1$^{1-36}$ (lanes 2-5), DBD-DSS1^{WT} (lanes 7-9), DBD-DSS1$^{1-54}$ (lanes 10-12), and DBD-DSS1^{R57Q} (lanes 13-15) at 90 mM KCl condition. Source data are provided as a Source Data file.

c. The quantification data (mean ± SD) from at least 3 independent experiments shown in Supplementary Fig. 8b. P values were calculated using two-way ANOVA for group comparison. **** P≤0.0001. Source data are provided as a Source Data file.
d. Representative gel of dsDNA (5 nM) binding by DBD-DSS1$^{1-36}$ (lanes 2-5), DBD-DSS1^{WT} (lanes 7-9), DBD-DSS1$^{1-54}$ (lanes 10-12), and DBD-DSS1^{R57Q} (lanes 13-15) at 90 mM KCl condition. Source data are provided as a Source Data file.
e. The quantification data (mean ± SD) from at least 3 independent experiments shown in Supplementary Fig. 8d. Source data are provided as a Source Data file.

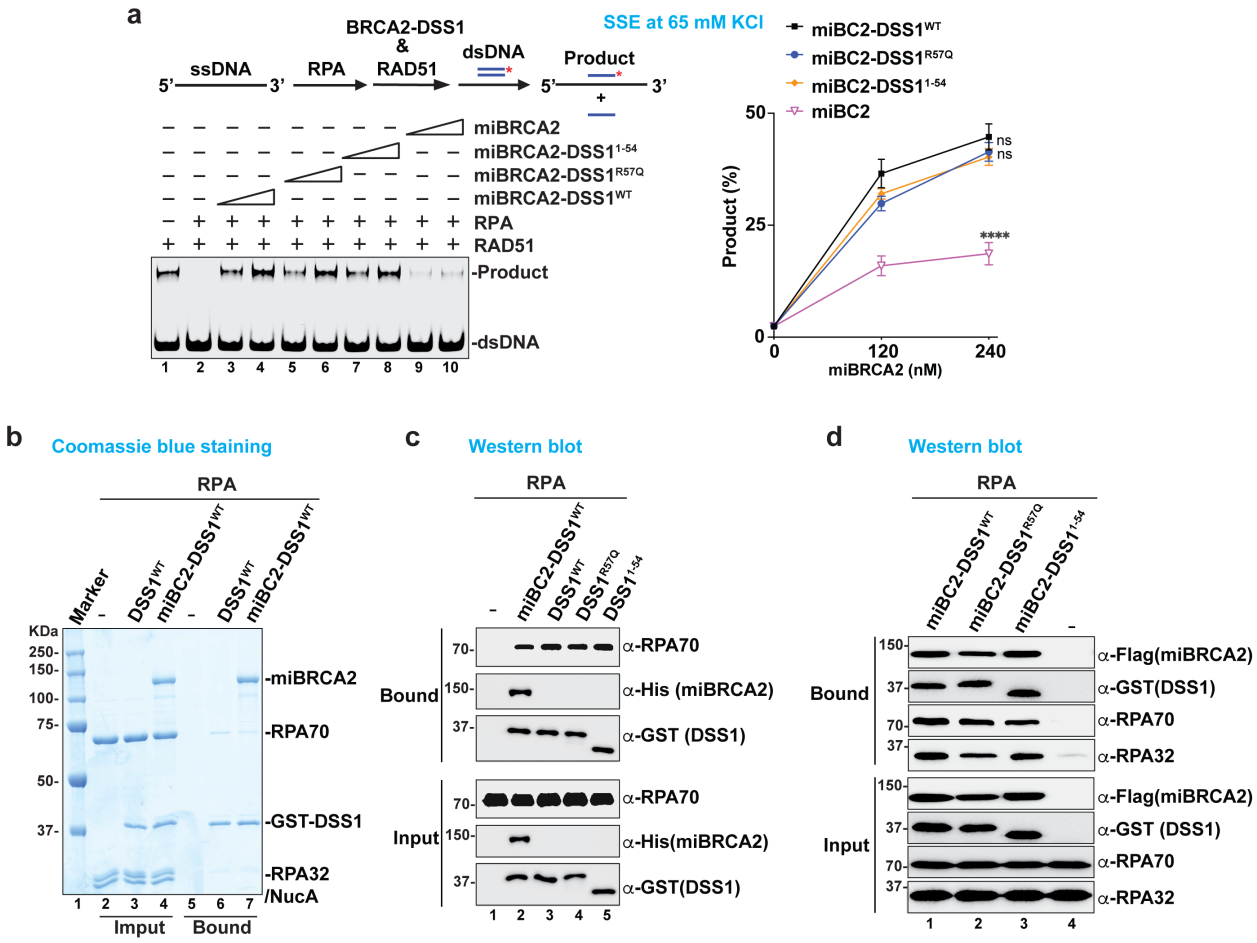

Supplementary Fig. 9. Recombination Mediator Activity of miBRCA2 with DSS1 or Mutants. (See also Fig. 3)
a. Schematic of homologous paring assay with ssDNA coated with RPA (top). The 120 and 240 nM miBRCA2-DSS1^{WT} (lanes 3-4), miBRCA2-DSS1^{R57Q} (lanes 5-6), miBRCA2-DSS1$^{1-54}$ (lanes 7-8) and miBRCA2 (lanes 9-10) were tested in homologous pairing reactions with ssDNA (20 nM) coated with RPA (150 nM, bottom) at the reaction with 65 mM KCl, Quantification (mean ± SD) of the homologous pairing product from three independent experiments shown on the right panel. P values were calculated using two-way ANOVA for group comparison. ns: not significant, ****

P≤0.0001. p value between miBC2-DSS1^{WT} and miBC2-DSS1^{R57Q} is 0.47, p value between miBC2-DSS1^{WT} and miBC2-DSS1$^{1-54}$ is 0.25, p value between miBC2 and miBC2-DSS1^{WT}/ miBC2-DSS1^{R57Q} /miBC2-DSS1$^{1-54}$ is <0.0001. Source data are provided as a Source Data file.
b. GST pull-down assay to test for the interaction of RPA with miBRCA2-DSS1^{WT} and GST-DSS1 in the presence of a non-specific DNA/RNA nuclease NucA at 150 mM KCl condition. The bound fractions of RPA (RPA70 and RPA32 subunits), miBRCA2 and GST-DSS1 among different complexes were analyzed by Coomassie Blue staining. Source data are provided as a Source Data file.
c. GST pull-down assay to test for the interaction of RPA with miBRCA2-DSS1^{WT}, GST-DSS1, GST-DSS1^{R57Q} and GST-DSS1$^{1-54}$ in the presence of a non-specific DNA/RNA nuclease NucA at 150 mM KCl condition. The bound fractions of RPA70, GST-DSS1 and miBRCA2 among different complexes were analyzed with α-RPA70, α-GST and α-His antibodies by Western blot analysis. Source data are provided as a Source Data file.
d. GST pull-down assay to test for the interaction of RPA with miBRCA2-DSS1^{WT}, miBRCA2-DSS1^{R57Q} and miBRCA2-DSS1$^{1-54}$ at 150 mM KCl condition. The bound fractions of RPA (RPA70 and RPA32 subunits), GST-DSS1 and miBRCA2 among different complexes were analyzed with α-RPA70, α-RPA32, α-GST and α-Flag antibodies by Western blot analysis. Source data are provided as a Source Data file.

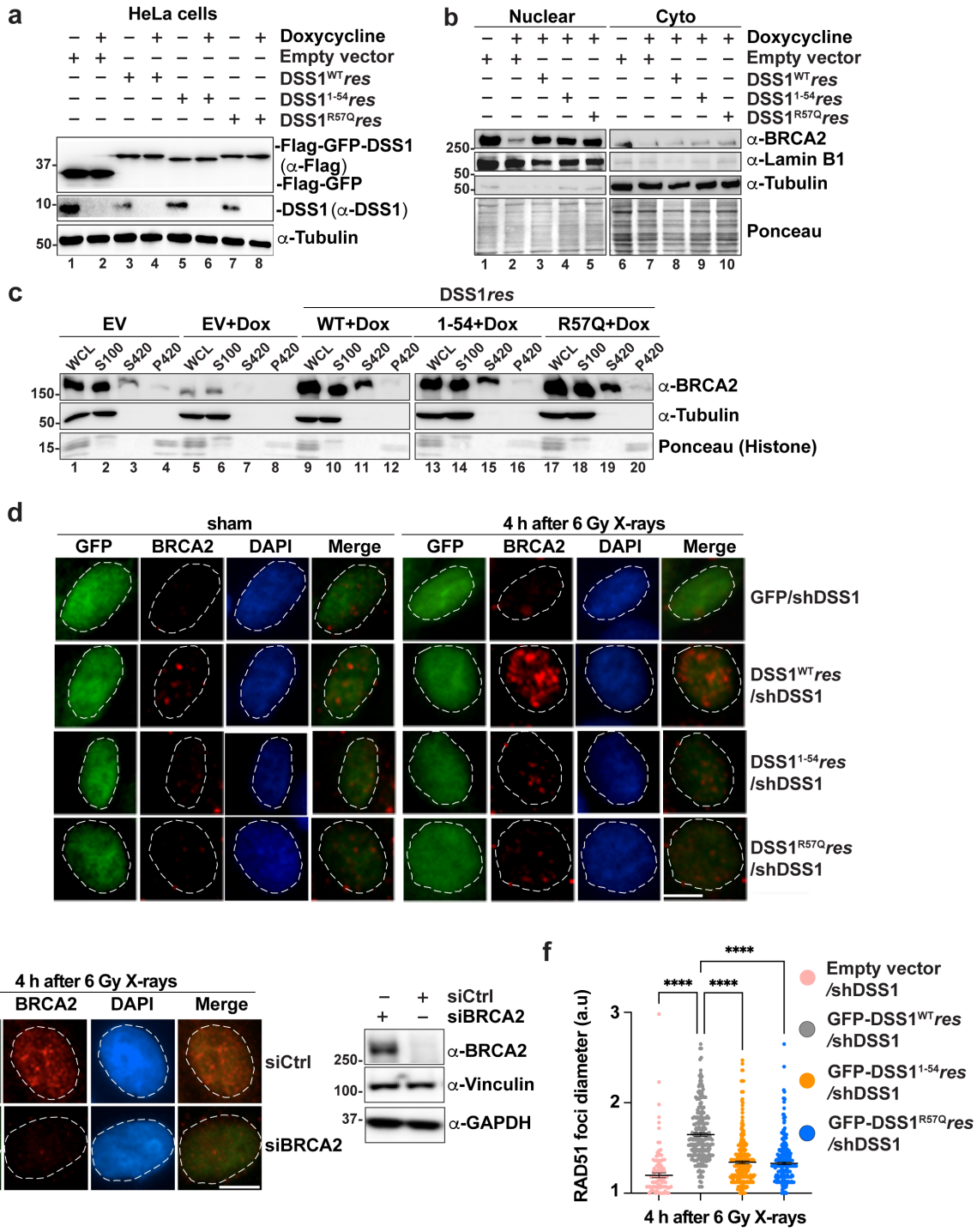

Supplementary Fig. 10. Characterization of Cells with Stable Expression of Wild-Type or Mutants of DSS1 in BRCA2/RAD51 nuclear localization and focus formation. (See also Fig. 4-6)

a. Representative Western blot analysis from three independent experiments to detect endogenous DSS1 and ectopic expression Flag-GFP-DSS1 in Hela cells expressing ectopic Flag-GFP-DSS1^{WT}*res*, Flag-GFP-DSS1$^{1-54}$*res*, or Flag-GFP-DSS1^{R57Q}*res* without or with endogenous DSS1

knockdown by doxycycline treatment. Tubulin was blotted as the loading control. Source data are provided as a Source Data file.
b. Representative Western blot from three independent experiments to examine the nuclear localization of BRCA2 in HeLa cells expressing ectopic Flag-GFP-DSS1^{WT}*res*, Flag-GFP-DSS1$^{1-54}$*res*, or Flag-GFP-DSS1^{R57Q}*res* with endogenous DSS1 knockdown by doxycycline. Lamin B1 and Tubulin act as a marker of the nuclear fraction and cytoplasmic fraction. The Ponceau S staining was shown as the loading control. Source data are provided as a Source Data file.
c. HeLa cells, which express ectopic Flag-GFP-DSS1^{WT}*res*, Flag-GFP-DSS1$^{1-54}$*res*, or Flag-GFP-DSS1^{R57Q}*res* with endogenous DSS1 knockdown by doxycycline and Olaparib treatment (10 μM, 24h), were further fractionated into NS100 (S100), NS420 (S420), and NP420 (P400). Whole cell lysate (WCL) was included. Tubulin was included as a marker of cytoplasmic fraction, while the Ponceau S staining was shown as the loading control for indication of histone in the nuclear. Representative Western blot is from three independent experiments. Source data are provided as a Source Data file.
d. Representative image of BRCA2 foci (red) in HeLa nuclei at 4hr after exposure to 6 Gy X-rays or sham irradiation from three independent experiments. Scale bar:10 μm.
e. Representative image of BRCA2 foci (red) in HeLa nuclei at 4hr after exposure to 6 Gy X-rays under the treatment of siControl or siBRCA2 from three independent experiments to verify the specificity of α-BRCA2 antibody, and Western blot analysis to detect endogenous BRCA2 blot in HeLa cells after treatment of siBRCA2, Vinculin and GAPDH were used as the loading control. Scale bar:10 μm. Source data are provided as a Source Data file.
f. Quantification (mean ± SD) of RAD51 foci diameter (corresponding to Fig. 4c) at 4hr after exposure to 6 Gy X-rays. P values were calculated using one -way ANOVA and Dunnett's multiple comparisons test. **** $P \leq 0.0001$. p-value between GFP-DSS1^{WT}res and EV/GFP-DSS1$^{1-54}$res /GFP-DSS1^{R57Q}res is <0.0001. Source data are provided as a Source Data file.

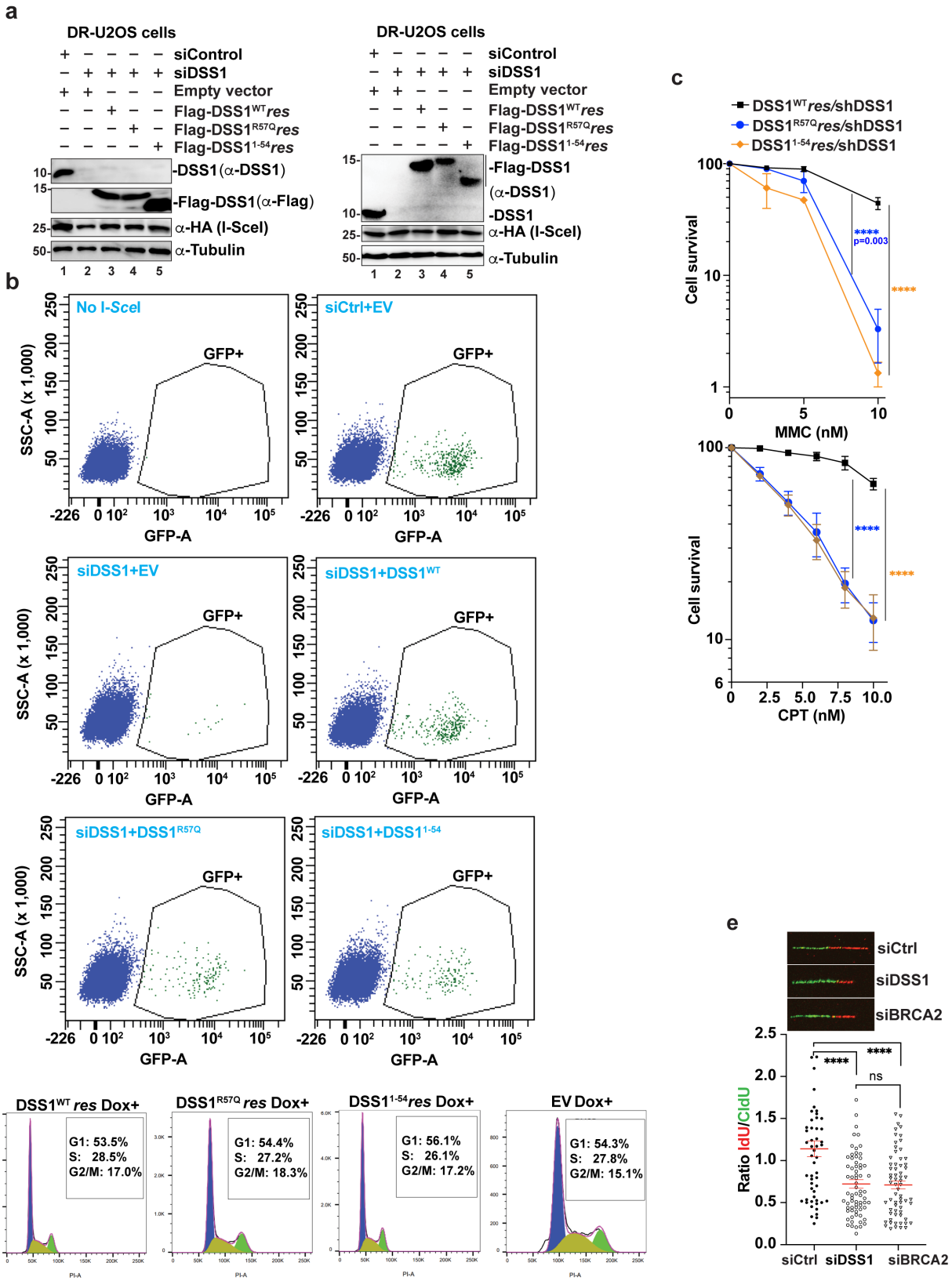
a
DR-U2OS cells
siControl
siDSS1
Empty vector
Flag-DSS1WTres
Flag-DSS1R57Qres
Flag-DSS1 1-54res
-DSS1(α-DSS1)
-Flag-DSS1(α-Flag)
α-HA (I-SceI)
α-Tubulin
DR-U2OS cells
siControl
siDSS1
Empty vector
Flag-DSS1WTres
Flag-DSS1R57Qres
Flag-DSS1 1-54res
-Flag-DSS1
(α-DSS1)
-DSS1
α-HA (I-SceI)
α-Tubulin
b
No I-SceI
siCtrl+EV
siDSS1+EV
siDSS1+DSS1WT
siDSS1+DSS1R57Q
siDSS1+DSS1 1-54
GFP+
SSC-A (x 1,000)
GFP-A
c
DSS1WTres/shDSS1
DSS1R57Qres/shDSS1
DSS1 1-54res/shDSS1
Cell survival
MMC (nM)
CPT (nM)
****
p=0.003
d
DSS1WT res Dox+
DSS1R57Q res Dox+
DSS1 1-54res Dox+
EV Dox+
G1: 53.5%
S: 28.5%
G2/M: 17.0%
G1: 54.4%
S: 27.2%
G2/M: 18.3%
G1: 56.1%
S: 26.1%
G2/M: 17.2%
G1: 54.3%
S: 27.8%
G2/M: 15.1%
e
siCtrl
siDSS1
siBRCA2
Ratio IdU/CldU
****
ns

Supplementary Fig. 11. Characterization of Cells with Stable Expression of Wild-Type or Mutants of DSS1 in HR and Survival. (See also Fig. 4-6)

a. Representative Western blot analysis to detect endogenous DSS1 in U2OS cells after treatment of DSS1 siRNA (α-DSS1) and transient expression level of ectopic Flag-DSS1$^{WT/R57Q/1-54}$ *res* (α-Flag) and I-SceI (α -HA) from three independent experiments. The anti-DSS1 antibody was used to check the endogenous (DSS1) and exogenous (Flag-DSS1) to compare the protein expression level. Source data are provided as a Source Data file.

b. Representative HR frequency of the assay with the DR-GFP reporter in U2OS cells.

c. Survival curves of HeLa cells with stable expression of GFP-DSS1^{WT}res, GFP-DSS1$^{1-54}$res or GFP-DSS1^{R57Q}res after the treatment with increasing concentrations of MMC or CPT. Endogenous DSS1 was depleted by doxycycline induced shDSS1 expression. The mean values (± SD) from three independent experiments were plotted. P values were calculated using two-way ANOVA for group comparison. ****P≤0.0001. Under the treatment of MMC, p value between GFP-DSS1^{WT}res and GFP-DSS1$^{1-54}$res is <0.0001, p value between GFP-DSS1^{WT}res and GFP-DSS1^{R57Q} res is 0.0029. Under the treatment of CPT, p value between GFP-DSS1^{WT}res and GFP-DSS1$^{1-54}$res is <0.0001, p value between GFP-DSS1^{WT}res and GFP-DSS1^{R57Q}res is <0.0001. Source data are provided as a Source Data file.

d**.** Cell cycle analysis of Hela-shDSS1 cells stably expressing wild-type or mutant Flag-GFP-DSS1 Symbol: EV, empty vector; Dox+, with doxycycline treatment.

e. Representative micrographs of fiber events in HeLa cells (top), where endogenous BRCA2 or DSS1 was depleted by siRNA against BRCA2 or DSS1, respectively. Dot plots of IdU to CIdU tract length ratios for individual replication forks in HU-treated cells (bottom). The median value of 50-70 CIdU and IdU tracts from three independent experiments. Data represent mean ± SEM. P values were calculated using one-way ANOVA for group comparison and Dunnett's multiple comparisons test. ns, not significant and **** P≤ 0.0001. p value between siCtrl and siDSS1 is <0.0001, p value between siCtrl and siBRCA2 is <0.0001, p value between siDSS1 and siBRCA2 is 0.98. Source data are provided as a Source Data file.

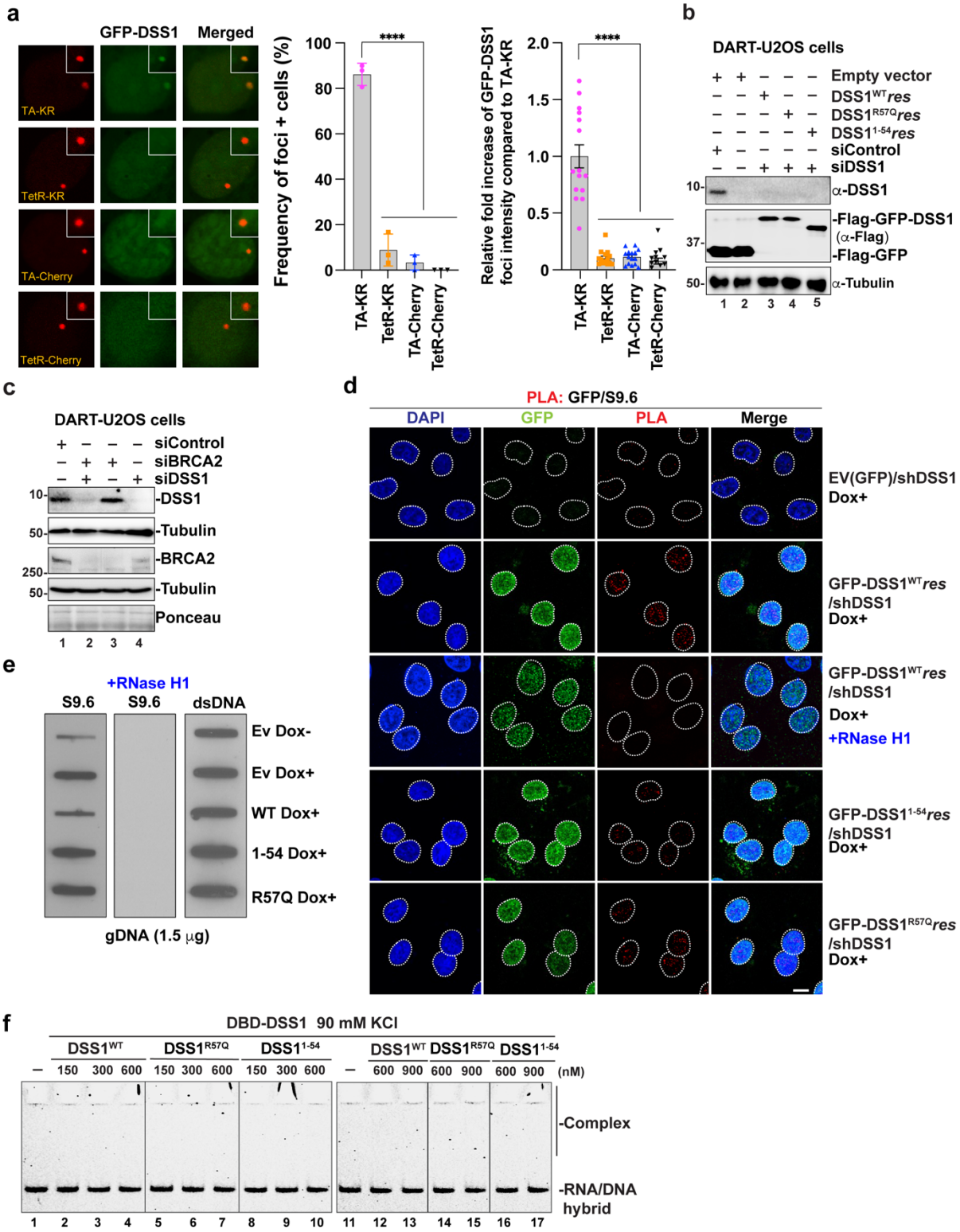

Supplementary Fig. 12. Examination of the Recruitment of DSS1 to the Sites of R-loops and Role of DSS1 C-terminal Helix in R-loop Accumulation. (See also Fig. 6)

a. U2OS-TRE cells transfected with pBROAD3 TetR-KR/Cherry or pBROAD3 TA-KR/Cherry and the expression vector of GFP-DSS1^{WT} were light-activated and recovered 20 min before fixation. Representative images of GFP foci recruitment at sites of TA-KR, TetR-KR, TA-Cherry or TetR-Cherry were shown (left). Foci-positive cells in each indicated group were quantified (n=30). The mean values ± SD of three independent experiments is shown (middle). Fold increase of GFP-DSS1^{WT} foci intensity of TA-KR, TetR-KR, TA-Cherry and TetR-Cherry compared to background was quantified (n=10, mean ± SD) (right). Statistical analysis was done with the Two-sided student-t-test, ns, not significant; ****P≤0.0001. (Left) p value between TA-KR and TetR-KR/TA-Cherry/TetR-Cherry is <0.0001. (Right) p value between TA-KR and TetR-KR/TA-Cherry/TetR-Cherry is <0.0001. Source data are provided as a Source Data file.

b. Representative Western blot analysis to detect ectopically expressed Flag-GFP-DSS1 and endogenous DSS1 after treatment of U2OS-TRE cells with DSS1 or control siRNA for the three independent experiments in Fig. 6 c and d. Tubulin was used as a loading control. Source data are provided as a Source Data file.

c. Representative Western blot analysis to detect endogenous BRCA2 and DSS1 after treatment of U2OS-TRE cells with BRCA2, DSS1 or control siRNA for the three independent experiments in Fig. 6 e. Tubulin and Ponceau S staining were used as a loading control. Source data are provided as a Source Data file.

d. Representative micrographs of PLA foci (red) of DSS1 (α-GFP) and R-loop (S9.6) in the nuclei of HeLa-shDSS1 cells stably expressing GFP-DSS1^{WT}res, GFP-DSS1$^{1-54}$res or GFP-DSS1^{R57Q}res after the treatment of CPT (10 μM; 2 h) with or without RNase H (10 units) treatment from three independent experiments. Blue: DAPI. Green, GFP-DSS1. The foci formation was analyzed over 200 cells using ImageJ. Symbol: EV, empty vector with GFP. Scale bar: 10 μm.

e. Representative RNA/DNA hybrid slot blot of genomic DNA from HeLa-shDSS1 cells stably expressing GFP-DSS1^{WT}res, GFP-DSS1$^{1-54}$res or GFP-DSS1^{R57Q}res after the treatment of CPT (10 μM; 2 h) from three independent experiments. RNA/DNA hybrid with or without RNase H treatment (10 units) was then probed with S9.6 antibody. dsDNA antibody was used for control input of each sample. Source data are provided as a Source Data file.